

Regression Models Using Shapes of Functions as Predictors

Kyungmin Ahn

RIKEN Center for Biosystems Dynamics Research (BDR), Japan

J. Derek Tucker

Sandia National Laboratories, Albuquerque, New Mexico, USA

Wei Wu, Anuj Srivastava

Florida State University, Tallahassee, Florida, USA

Abstract

Functional variables are often used as predictors in regression problems. A commonly-used parametric approach, called *scalar-on-function regression*, uses the \mathbb{L}^2 inner product to map functional predictors into scalar responses. This method can perform poorly when predictor functions contain undesired phase variability, causing phase changes to have disproportionately large influence on the response variable. One past solution has been to perform phase-amplitude separation (as a pre-processing step) and then apply functional regression model. Here we propose a more integrated approach, termed *elastic functional regression model* (EFRM), where phase-separation is performed inside the regression model, rather than as pre-processing. This approach generalizes the notion of phase in functional data, and is based on the norm-preserving warping of predictors. Due to its superior invariance properties, this representation provides robustness to phase components and results in improved predictions of the response variable over traditional models. We demonstrate this framework using a number of datasets involving gait signals and historical stock market prices.

Keywords: functional data analysis, functional regression, functional single-index model, function alignment

1. Introduction

A fast growing subtopic in functional data analysis (FDA) [1] is *regression* involving functional variables, either as predictors or responses or both. Morris [2] categorizes regression problems involving functional data into three types: (1) functional predictor regression (scalar-on-function), (2) functional response regression (function-on-scalar) and (3) function-on-function regression. The functional predictor regression problem (or scalar-on-function) model was first studied by Ramsay [3], Cardot et al. [4], and several other since then [5–12]. Here the predictors are scalar functions over a fixed interval say $[0, T]$, call them $\{f_i \in \mathcal{F}\}$, elements of some pre-specified functional space \mathcal{F} , and the response variables are scalar random variables $\{y_i \in \mathbb{R}\}$. (One can easily extend this framework to the case where functions are vector-valued.) A simple and commonly-used model for this problem is the so-called *functional linear regression model* (FLM) given by:

$$y_i = \alpha + \langle \beta, f_i \rangle + \epsilon_i, \quad i = 1, \dots, n, \quad (1)$$

where $\alpha \in \mathbb{R}$ is the intercept, $\beta \in \mathcal{F}$ is the regression-coefficient function, and $\epsilon_i \in \mathbb{R}$ is the observation noise. Also, $\langle \beta, f_i \rangle$ denotes the standard \mathbb{L}^2 inner product $\int_0^T f_i(t)\beta(t) dt$. (Notationally, we will use $\|\cdot\|$ to denote the \mathbb{L}^2 norm.) One assumes here that \mathcal{F} has the \mathbb{L}^2 Hilbert structure to allow for this inner product between its elements. Similar to linear regression models with Euclidean variables, one can also estimate model parameters here by minimizing the sum of squared errors (SSE):

$$\{\hat{\alpha}, \hat{\beta}\} = \underset{\alpha \in \mathbb{R}, \beta \in \mathbb{L}^2}{\operatorname{argmin}} \left[\sum_{i=1}^n (y_i - \alpha - \langle \beta, f_i \rangle)^2 \right]. \quad (2)$$

However, since \mathbb{L}^2 is infinite dimensional, this problem is not sufficiently constrained for estimating $\hat{\beta}$ with a finite n , and requires further restrictions. These constraints can come in form of a regularization term or by restricting the solution space, or both. For restricting the solution space, one can use a complete orthonormal basis of \mathcal{F} , for representing β via its coefficients, and then truncate it to make the representation finite dimensional. A regularization is often imposed using a roughness measure on β , e.g. $\int \ddot{\beta}(t)^2 dt$. (Given a function $f(t)$, we will use $\dot{f}(t)$ and $\ddot{f}(t)$ to denote the first and the

second derivative of $f(t)$, respectively.) The FLM model can easily be extended to a *generalized functional linear model* [13], where the conditional mean of the response given the predictors uses a known link function.

1.1. Basic Issue: Predictor Phase

While the use of functional data has grown in recent years, there has also been a growing awareness of a problem/issue that is specific to such data. Functional data most often comes with a *phase variability*, i.e. a lack of registration between geometric features (peaks, valleys, etc) across functions [14–16]. This situation arises, for example, when using bio-signals, growth curves, or stock market data, and where measurements across experiments lack temporal synchronizations. Different functional measurements can potentially have different temporal rates of evolutions, introducing an intrinsic phase variability in the data. In mathematical terms, the functional data is not $\{f_i\}$, as in the original model, but observed under some random action of Γ , the group of all time warping functions. In fact, there are different types of actions possible, depending on the context.

- **Value-preserving warping:** The most commonly used mapping is $f_i \mapsto (f_i \circ \gamma_i)$ is called *value-preserving warping* as it preserves the values of f_i and only shifts them horizontally. It is often used in alignment of peaks and valleys in functional data.
- **Area-preserving warping:** The mapping $f_i \mapsto (f_i \circ \gamma_i)\dot{\gamma}_i$, is called an *area-preserving warping*, since it preserves the area under the curve f_i . It is often used when $\{f_i\}$ are probability density functions.
- **Norm-preserving warping:** Another kind of warping comes from the mapping $f_i \mapsto (f_i \circ \gamma_i)\sqrt{\dot{\gamma}_i}$, called an *norm-preserving warping*, since it preserves the \mathbb{L}^2 -norm of f_i . That is, $\|f_i\| = \|(f_i \circ \gamma_i)\sqrt{\dot{\gamma}_i}\|$ for all $f_i \in \mathbb{L}^2$ and $\gamma \in \Gamma$.

Additional warpings may also be utilized in a model, depending on the context. While in functional data alignment one mainly uses the value-preserving warping of functions, we will **keep the notion of phase more general in this paper**. Since our goal

is regression and prediction, instead of just functional alignment, we are free to try different actions as needed. In the following, we will use $(f_i^* \gamma_i)$ as a general notation for any one of these warpings.

In analysis and modeling of functional data, it is often advantageous to take into account explicitly the action of Γ on the functional data – for analysis [14–16] and for modeling [17]. For instance, a common idea in FDA is to perform alignment of peaks and valleys across functions using the value-preserving warpings $(f_i^* \gamma_i = f_i \circ \gamma_i)$ of their domains. These warpings $\{\gamma_i\}$ correspond to the phase components and the aligned functions $\{f_i \circ \gamma_i\}$ correspond to the shape or amplitude components. To illustrate these concepts, consider the two examples shown in Fig. 1. On the left we see the *Tecator* data which shows curves of absorbance of certain meat material and has been used commonly in many functional regression papers. The predictor functions here are already well registered and one can use them directly in a statistical model without any consideration of phase or phase separation. The right side shows a different situation involving the famous *Berkeley growth* data, where the growth velocities of 69 male subjects are displayed in the middle panel. While these curves have a similar number of peaks and valleys, these features are not well aligned across subjects, due to different growth rates and body clocks of subjects. This data contains a large phase variability and phase separation becomes important for statistical analysis. The result of a phase-amplitude separation algorithm [16] applied to the data is shown in the right panel.

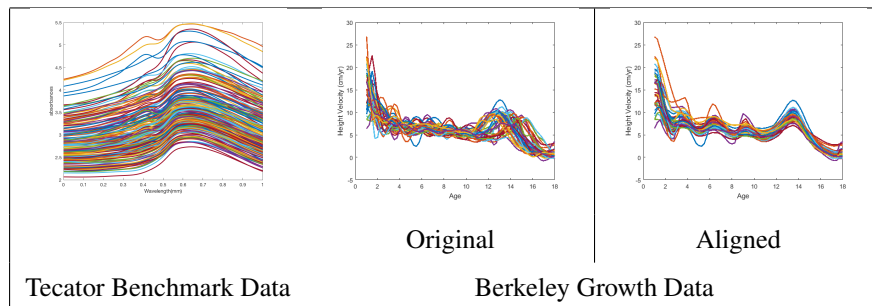


Figure 1: Example of functional data with and without phase variability.

One may envision functional regression models where both the components – phase and shape – are both treated as predictors. However, there are some other situations where only one of them, most notably, the shape of the function, is of interest in predicting a response variable. This situation arises, for instance, in cases where the response depends primarily on the number and heights of the modes in the predictor functions, but the locations of these modes and anti-modes play a lesser role and are considered nuisance. For example, in growth data, imagine a certain response variable, say the gender of the subject, that depends primarily on the shapes of these curves and not on the locations of growth spurts. Thus, shape-based functional regression becomes a useful tool in this context. Motivated by such problems, we shall develop a regression model where only the shape (or amplitude) of a function is considered as a predictor and its phase is removed from the consideration.

The phase variability in functional predictors, even if small, can have a disproportionately large influence on statistical analysis. One consequence of phase variability is the inflation of variance in the predictor itself, i.e. the variance of $\{f_i^* \gamma_i\}$ can be much higher than that of $\{f_i\}$, rendering any ensuing variance-based analysis ineffective. Another consequence is in the regression setup itself. Under the value-preserving warping, using the Taylors' expansion, we get

$$f_i(\gamma_i(t)) = f_i(t) + \dot{f}_i(t)(\gamma_i(t) - \gamma_{id}(t)) + \text{higher order terms} ,$$

with $\gamma_{id}(t) = t$. Dropping the higher-order terms and replacing f_i by $f_i \circ \gamma_i$ in Eqn. 1, we get

$$E[y_i | \beta, f_i] = \alpha + \langle \beta, f_i \rangle + \langle \beta, \dot{f}_i(\gamma_i - \gamma_{id}) \rangle .$$

The conditional mean gets changed, up to the first order, by an amount captured by the third term on the right side. Depending on the value of \dot{f}_i s, this value can be large, adversely affecting the prediction performance. While this discussion involved value-preserving time warping, a similar analysis can also be done for other group actions also, with similar conclusions. Sometimes these misalignments or phase variability are simple linear or affine shifts, and can be handled more easily, but in general the misalignments are nonlinear and one requires more comprehensive mathematical tools.

We further illustrate the issue of phase variability in regression models using a simulated example. Specifically, we quantify the deterioration in response prediction performance as the amount of random warping in the predictor functions is increased. The results are shown in Fig. 2. The left panel shows examples of predictors $\{f_i\}$ used in these experiments. For a fixed β we simulate responses y_i s using Eqn. 1, and use the data $\{(f_i, y_i), i = 1, 2, \dots, 100\}$ to estimate the model parameters including $\hat{\beta}$. Next, using this estimated $\hat{\beta}$, we want to predict the response variable for test predictors. However, in the test data we use predictors that are now *contaminated by time-warping* in two different ways: (i) $\{\tilde{f}_i = f_i \circ \gamma_i\}$, and (ii) $\{\tilde{f}_i = (f_i \circ \gamma_i)\sqrt{\gamma_i}\}$. Ignoring this contamination and using a standard predictor, we obtain predictions and quantify the prediction performance using the coefficient of determination R^2 . Specifically, we study the changes in R^2 as the amount of warping noise increases. The warping functions used in this experiment are given by $\gamma_i(t) = t + \alpha_i t(1 - t)$, where $\alpha_i \sim U(-a, a)$; the larger the value of a , the larger is warping noise. The bottom panels show examples of warping functions for different values of a . The middle and the last panels in the top row show plots of R^2 versus a (averaged over 200 runs) for the two different warping maps. In either case we observe a super linear decay in the performance. These experiments underline the fact that even a small amount of phase variability in predictors, either value-preserving or norm-preserving, can lead to a significant deterioration in prediction performance. Thus, one needs to account for this variability inside the model itself in an intrinsic way.

We reiterate that phase is a nuisance variable in some applications, but not in all situations. One should not always expect the shapes of predictor functions to be predominant in prediction. Phase components may also carry important information about the responses and one can not always ignore them. However, in some cases, as illustrated through examples presented later in this paper, shape can be the primary predictor and one wants models that can exploit this knowledge.

1.2. Potential Solutions

This leads us to an important question: *What kind of regression models allow dependence only on the shape or amplitude of the predictor functions and deemphasizes*

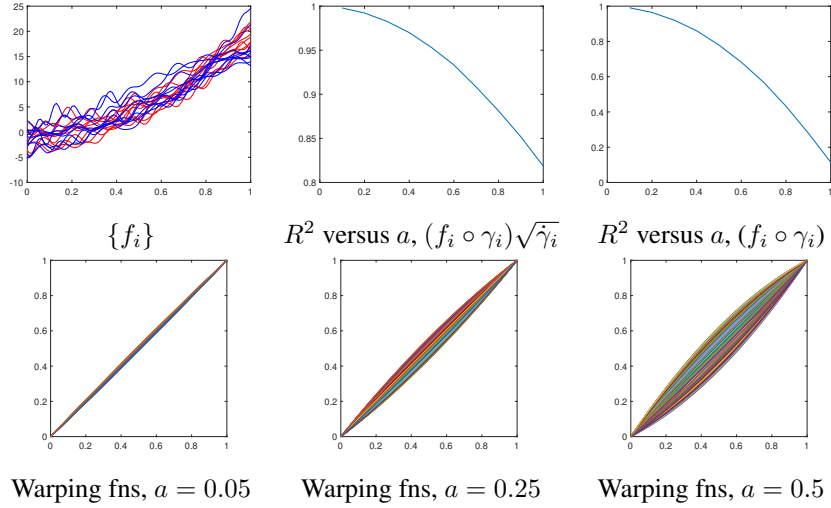


Figure 2: Experiments show approximately quadratic decrease in R^2 prediction measure as the amount of phase variability is increased in predictor functions.

their phases? In general there are both parametric and nonparametric choices, some of which we list below:

1. **Pre-Aligned Functional Linear Model (PAFLM):** One obvious solution is to simply remove the phase variability in the given functions $\{f_i\}$, using one of several pre-existing functional alignment algorithms (see e.g. [16–19]). Then, use the aligned functions, or amplitudes, for predicting the response variable using FLM. These are typically based on aligning the given $\{f_i\}$ one-by-one to a template function which, in turn, is constructed iteratively using the means of the aligned functions. The limitation of this approach in regression setting is that this alignment is performed independent of the response variable. In other words, the values $\{y_i\}$ do not play any role in optimizing over the phase variability.
2. **Joint Modeling & Alignment Under Value-Preserving Warping Using the \mathbb{L}^2 Inner-Product:** Another possibility is to remove the phase variability within an FLM model by including phase as a nuisance variable. For instance, when using the contaminated predictors $\{\tilde{f}_i = f_i \circ \gamma_i\}$, under the value-preserving warping, one can try to solve for the unknown warping functions by adding one

more optimization. That is, we can modify the model in Eqn. 1 to become:

$$y_i = \alpha + \sup_{\gamma_i} \left(\int_0^T \tilde{f}_i(\gamma_i(t)) \beta(t) dt \right) + \epsilon_i, \quad i = 1, \dots, n. \quad (3)$$

This additional optimization over Γ is supposed to nullify the original contamination in f_i s. However, this approach as specified has a major shortcoming. As described in several places, see e.g. Marron et al [15] and Srivastava-Klassen [20], the optimization over γ_i under the \mathbb{L}^2 is actually degenerate, due to a phenomenon called the *pinching effect*. Some authors minimize pinching by restricting the set of warpings in Eqn. 3 in a pre-determined manner. This restriction is unnatural as it is mostly impossible to pre-determine the optimal set of warpings needed to align future data.

3. **Nonparametric Regression Model:** Nonparametric models for functional regression are gaining popularity since they do not require any predetermined model and are purely data driven. Developed and studied by Ferraty and Vieu [21] and several others, one nonparametric model is given by: $y_i = G(f_i) + \epsilon_i$, where G is the unknown smooth map from \mathcal{F} to \mathbb{R} , and is estimated by the functional Nadaraya-Watson (NW) estimator [22]. For the given data (f_i, y_i) for $i = 1, 2, \dots, n$, the estimator is given by:

$$\hat{G}(f) = \frac{\sum_{i=1}^n y_i K(d(f_i, f)/b)}{\sum_{i=1}^n K(d(f_i, f)/b)}, \quad (4)$$

where: K is the standard Gaussian kernel, b is a positive scalar, and d is a chosen distance on the predictor (function) space. Naturally, the choice of distance d is critically important in such kernel estimators. If we use the standard \mathbb{L}^2 norm in \mathcal{F} as d , then the prediction will remain dependent on the phase components of the predictors. Instead, if we choose a distance between the *shapes of the predictor functions* as d , i.e. a proper shape metric, then model will be invariant to the phase components.

1.3. Proposed Approach

There is possibility of a different parametric approach by modifying the main term in the functional linear model directly, and making it invariant to the phase component

of the predictor. We develop a novel solution that is motivated by the use of invariant metrics, such as the Fisher-Rao metric and the elastic Riemannian metric in functional data alignment [16, 20]. In fact, depending on the chosen group action of Γ , this elastic functional data analysis framework suggests several ideas, although only a couple of them are discussed here. This framework is based on replacing the \mathbb{L}^2 inner product and the \mathbb{L}^2 distance between functions by invariant Riemannian metrics and invariant distances between functions. The invariant quantities provide better mathematical and numerical properties, and indeed lead to a superior registration between functions. The challenge in using the original invariant metric comes from its complicated expression, but that is overcome using the square root velocity function (SRVF) (Srivastava et al. [16]) defined as: $q(t) = \text{sign}(\dot{f}(t))\sqrt{|\dot{f}(t)|}$. One works with the SRVFs q_i s instead of the predictors f_i s and an invariant metric simplifies to the standard \mathbb{L}^2 metric. This framework motivates at least two ways of fixing the problem in Eqn. 3:

1. **Use SRVF Representation and Value-Preserving Warping:** The first idea is to compute SRVFs of the given predictors, and then simply replace the term $\sup_{\gamma_i} \langle f_i \circ \gamma_i, \beta \rangle$ in Eqn. 3 by the term: $\sup_{\gamma_i} \langle (q_i \circ \gamma_i)\sqrt{\dot{\gamma}_i}, \beta \rangle$. This is motivated by the fact that under a certain invariant metric, the inner product between functions is exactly equal to the \mathbb{L}^2 inner product. Under SRVF representation, the time warpings of q_i s, given by $(q_i \circ \gamma_i)\sqrt{\dot{\gamma}_i}$, are norm preserving. That is, $\|q_i\| = \|(q_i \circ \gamma_i)\sqrt{\dot{\gamma}_i}\|$ for all $q_i \in \mathbb{L}^2$ and $\gamma_i \in \Gamma$, and thus pinching is no longer possible. More importantly, the model is now completely independent of the phase components of the predictors f_i s.
2. **Use Original Functions and Norm-Preserving Warping:** The other option is to incorporate the norm-preserving action of the functions themselves ($f_i \mapsto (f_i \circ \gamma_i)\sqrt{\dot{\gamma}_i}$). As noted earlier, this warping changes both the locations and the heights of peaks and valleys in function, but preserve its \mathbb{L}^2 norm. With this choice, we use the term $\sup_{\gamma_i} \langle (f_i \circ \gamma_i)\sqrt{\dot{\gamma}_i}, \beta \rangle$ to replace the problematic \mathbb{L}^2 inner-product term in Eqn. 3. This option is especially useful when the predictor functions are noisy and an SRVF transformation may further enhance this noise by taking a derivative. By treating f_i s as SRVFs, one inherits all the nice proper-

ties of this framework and avoids enhancing the noise. However, this warping is different from the value-preserving warping $f \circ \gamma_i$ used in functional alignment. Thus, these γ_i s can be called *phase* only in a broader sense but not in a classical sense. In the end, the regression model is invariant to the phase of the predictors, except the phase is defined using the mapping $f_i \mapsto (f_i \circ \gamma_i)\sqrt{\dot{\gamma}_i}$ this time.

Each of these models help remove the phase variability, avoid the pinching effect, and improve prediction performance. Ultimately, the choice of a model depends on the nature of the data and the goals of the application. The response variables in both these models are invariant to respective time warpings of the predictor functions. In this paper, we will develop the second approach and will call this the *elastic functional regression* (EFRM) model.

The rest of this paper is as follows. In Section 2, we develop the resulting elastic functional regression model and discuss estimation of model parameters. We demonstrate this model using some simulated data and real data, and compare its performance against some current ideas in Section 3. Lastly, Section 4 ends the paper with some concluding remarks.

2. Elastic Functional Regression Model (EFRM)

2.1. Model Specification

In this section, we layout a regression model for *scalar-on-function* problem with the property that the response variable is invariant to the phase component of the predictor. This framework is based on ideas used previously for alignment of functional data, or phase-amplitude separation, using invariant metrics and the SRVF representation of functions. We start by briefly introducing those concepts and refer the reader to [16] for additional details.

As mentioned earlier, the use of \mathbb{L}^2 inner-product or \mathbb{L}^2 norm for alignment of functions leads to a well-known problem called the *pinching effect*. While some papers avoid this problem using a combination of external penalties and search space reductions, a more comprehensive solution comes from using an elastic Riemannian

metric with appropriate invariance properties. This metric, called the *Fisher-Rao metric* for functions, avoids the pinching effect without any external constraint and results in superior alignment results. Let f be a real-valued function on the interval $[0, 1]$ (with appropriate smoothness) and let \mathcal{F} denote the set of all such functions. For the purpose of alignment, one represents it using a square-root velocity function (SRVF): $q(t) = \text{sign}(\dot{f}(t))\sqrt{|\dot{f}(t)|}$. One of the advantages of using SRVF is that under the transformation $f \mapsto q$, the complicated Fisher-Rao Riemannian metric and the Fisher-Rao distance into much simpler expressions (\mathbb{L}^2 metric and \mathbb{L}^2 norm, respectively). If we warp a function f by a time warping γ , i.e., map $f \mapsto (f \circ \gamma)$, then its SRVF changes by $q \mapsto (q \circ \gamma)\sqrt{\dot{\gamma}}$. The latter is often denoted by $(q * \gamma)$. The invariance property of the Fisher-Rao metric implies that for any $q_1, q_2 \in \mathbb{L}^2$ and $\gamma \in \Gamma$, we have: $\|(q_1 * \gamma) - (q_2 * \gamma)\| = \|q_1 - q_2\|$. In other words, the action of Γ on \mathbb{L}^2 is by isometries. A special case of this equation is that $\|(q * \gamma)\| = \|q\|$ for all q and γ . Thus, this action preserves the \mathbb{L}^2 norm of the SRVF and, therefore, avoids any pinching effect.

This framework motivates several solutions for avoiding the pinching problem associated with the inner-product term in Eqn. 3. While one can work with the SRVFs of the given predictor functions, they are prone to noise in the original data due to the involvement of a time derivative in the definition of SRVF. In case the original data is noisy, this noise gets enhanced by taking a derivative. As a workaround to this problem, we treat the given predictor functions to be in the SRVF space already. That is, we assume the action of warping γ_i on an f_i s is given by $(f_i \circ \gamma_i)\sqrt{\dot{\gamma}_i}$ and not $f_i \circ \gamma_i$. With this action, we have that $\|(f_i * \gamma_i)\| = \|(f_i \circ \gamma_i)\sqrt{\dot{\gamma}_i}\| = \|f_i\|$.

Based on this argument, the inner-product term in Eqn. 3 can be replaced by the term: $\sup_{\gamma_i} \langle \beta, (f_i * \gamma_i) \rangle$. This is a scalar quantity and represents a modified linear relationship between the predictor and the response. One can impose a single-index model on top of this construction to generalize this model. Such single-index models have been used commonly in conjunction with the Functional Linear Model (FLM), see e.g. [7, 23–26]. For any $h : \mathbb{R} \rightarrow \mathbb{R}$, a smooth function, define EFRM the model:

$$y_i = h\left(\sup_{\gamma_i} \langle \beta, (f_i * \gamma_i) \rangle\right) + \epsilon_i, i = 1, \dots, n \quad (5)$$

To complete model specification, we assume ϵ_i s to be *i.i.d* zero-mean, Gaussian ran-

dom variables.

This model has the following properties.

1. **Nonlinear Relationships:** There are two sources of nonlinearity in the relationship between f_i and y_i . Although the inner product $\langle \beta, f_i \rangle$ is linear in f_i , the supremum over Γ makes the term $\sup_{\gamma_i} \langle \beta, (f_i * \gamma_i) \rangle$ nonlinear. Furthermore, the inclusion of h allows EFRM to capture nonlinear relationships between the predictor and the response variables.
2. **Invariance to Phase:** For a fixed model description (β, h) , the contribution of f_i is invariant to its component γ_i due to the fact that $\sup_{\gamma_i} \langle \beta, (f_i * \gamma_i) \rangle = \sup_{\gamma_i} \langle \beta, ((f_i * \gamma_0) * \gamma_i) \rangle$, for all $\gamma_0 \in \Gamma$. Even though the response is invariant to the phase, we note that the estimated values of β and h (covered in the next section) are actually dependent on the phase variability in f_i s.
3. **Specification of β :** In view of the equality mentioned in the previous item, the regression coefficient is not fully specified. This is because if $\hat{\beta}$ is an estimator of β , then so is $\hat{\beta} \circ \gamma$ for any $\gamma \in \Gamma$. To avoid this ambiguity we impose an additional constraint on the model that all the maximizers $\{\hat{\gamma}_i = \arg \sup_{\gamma_i} \langle \beta, (f_i * \gamma_i) \rangle\}$ together satisfy the condition that $\frac{1}{n} \sum_{i=1}^n \hat{\gamma}_i = \gamma_{id}$.
4. **Different from GFLM:** The single-index model used here is quite similar to a generalized functional linear model, but with an important difference. In a single-index model, the index function h is unknown and needs to be estimated from the data itself, while in generalized model h is assumed known. One can also easily switch to generalized model in our framework by using a known h .

2.2. Parameter Estimation

Next we consider the problem of estimating EFRM parameters using MLE. The list of unknown parameters includes the index function h and the coefficient of regression β . We take an iterative approach, laid out in [27], where one updates the estimates of h or β while keeping the other fixed. Thus, we first focus on techniques for estimating these quantities separately.

Estimation of β Keeping h Fixed. : Given a set of observations $\{(f_i, y_i)\}$, the goal here is to solve for the coefficient of regression β , while keeping h fixed, using maximum-likelihood estimation. In order to reduce the search space to a finite-dimensional set, we will assume that $\beta \in \{\sum_{j=1}^J c_j b_j | c_j \in \mathbb{R}\}$ for a fixed basis set $\mathcal{B} = \{b_j, j = 1, 2, \dots\}$ of $\mathbb{L}^2([0, 1], \mathbb{R})$. The estimation problem is now given by:

$$\hat{c} = \underset{c \in \mathbb{R}^J}{\operatorname{argmin}} H(c), \text{ where } H : \mathbb{R}^J \rightarrow \mathbb{R},$$

$$H(c) = \left(\sum_{i=1}^n (y_i - h(\sup_{\gamma_i} \left\langle \sum_{j=1}^J c_j b_j, (f_i * \gamma_i) \right\rangle))^2 \right).$$

We use an optimization function available in matlab software for this. Contained in the optimization over $c \in \mathbb{R}^J$ are a set of optimizations over γ_i s. For a fixed c , this optimization is performed using the dynamic programming algorithm (DPA) for each $i = 1, 2, \dots, n$. This set of calls to DPA are inside the definition of H and are performed for each candidate value of c . Thus, any update of c requires recomputing the optimal warping functions, resulting in an iterative process. Finally, once c or β is estimated, we can impose the condition for specification of β , i.e. $\frac{1}{n} \sum_{i=1}^n \hat{\gamma}_i = \gamma_{id}$ as follows. For this, we use the current $\hat{\gamma}_i$ s to compute their average $\bar{\gamma} = \frac{1}{n} \sum_{i=1}^n \hat{\gamma}_i$ and replace β by $\beta \circ \bar{\gamma}^{-1}$.

The process of estimating β is summarized in Algorithm 1.

To analyze this estimation, one has to study the choice of J relative to the sample size n , and develop an asymptotic theory for this estimator. Since this analysis is very similar to existing papers on involving functional predictors [28, 29], we simply refer to that literature for asymptotic analysis.

Estimation of h Keeping β Fixed. Next we consider the problem of estimating the index function h given the data and the current estimate of β . The reason for introducing this single-index model is to capture nonlinear relationship between the predicted responses and observed responses. While there are many potential nonparametric estimators for h , we keep the model simple by restricting to lower-order polynomials. Hence, this index function can either be linear, quadratic, cubic, and so on: $h(x) = ax + b$, $h(x) = ax^2 + bx + c$, and $h(x) = ax^3 + bx^2 + cx + d$, etc. In the experiments presented

Algorithm 1 Estimation of β keeping h fixed

- 1: Initialization Step. Choose an initial $c \in \mathbb{R}^J$ and compute $\hat{\beta}(t) = \sum_{j=1}^J c_j b_j(t)$.
 - 2: Use an optimization code (such as `fminunc` in matlab) to find \hat{c} that minimizes the cost function H .
 - To define H , use the current \hat{c} (and $\hat{\beta}$) to perform the following for each $i = 1, 2, \dots, n$,
 - Solve for $\hat{\gamma}_i = \operatorname{argmin}_{\gamma \in \Gamma} \|\hat{\beta} - (f_i * \gamma)\|^2$, using the Dynamic Programming algorithm (DPA).
 - Compute the aligned functions $\tilde{f}_i \leftarrow (f_i * \gamma_i) \equiv (f_i \circ \hat{\gamma}_i) \sqrt{\dot{\hat{\gamma}}_i}$.
 - 3: Update $\hat{\beta}(t) = \sum_{j=1}^J \hat{c}_j b_j(t)$. If the $|H(\hat{c})|$ is large, then return to step 2.
 - 4: Compute $\bar{\gamma} = \frac{1}{n} \sum_{i=1}^n \hat{\gamma}_i$ and replace β by $\beta \circ \bar{\gamma}^{-1}$.
-

later, we use only the first three polynomial functions for h .

For estimating h , we first predict responses according to: $\hat{y}_i = \sup_{\gamma_i} \langle \hat{\beta}, (f_i * \gamma_i) \rangle$, and then we fit a polynomial function h between the predicted responses \hat{y}_i and the observed responses y_i using the least squares error criterion. The full parameter estimation procedure is as presented in Algorithm 2.

Algorithm 2 Elastic Functional Regression Model

- 1: Initialize h as the identity function ($h(x) = x$).
 - 2: Given h , use Algorithm 1 to estimate $\hat{\beta}$.
 - 3: For a given $\hat{\beta}$, fit the single-index model using the least squares criterion and update h .
 - 4: If $|H(\hat{c})|$ is small, then stop. Else, return to step 2.
-

2.3. Prediction of Response Under the Elastic Regression Model

One of the goals of EFRM is to predict values of the response variable for the future predictor observations. Next we describe a prediction process under EFRM. This process involves aligning the predictors to the coefficient $\hat{\beta}$ using DPA. For a

given predictor $f^{(test)}$, the predicted value of y is:

$$\hat{y} = \hat{h} \left(\sup_{\gamma_i} \left\langle \sum_{j=1}^J \hat{c}_j b_j, (f^{(test)} * \gamma_i) \right\rangle \right). \quad (6)$$

We will use this predictor to evaluate the prediction of EFRM, relative to other current models, using both simulated data and real data.

3. Experimental Illustration

In this section, we compare our method with four natural alternatives. Either these models are commonly used in the literature or they are simple modifications of the current models for handling the phase variability in the predictors. These models are: Functional Linear Model (FLM); Pre-Aligned Functional Linear Model (PAFLM); Nonparametric regression model (NP) using a Gaussian kernel function and two different functional distances: \mathbb{L}^2 distance and elastic shape distance. We briefly summarize and introduce these models.

Functional Linear Model (FLM). Functional Linear Model has already been introduced in Eqn. 1. As stated earlier, it does not specifically account for the presence of phase variability in the predictor data and is vulnerable to that nuisance variability.

Pre-Aligned Functional Linear Model (PAFLM). PAFLM is the model where one pre-aligns the predictor functions (using a phase-amplitude separation algorithm) and then performs standard FLM. To clarify further, one performs phase-amplitude separation and then discards the phase component. For instance, the registration can be implemented using SRVFs and *template function or karcher mean* as stated in the “*Complete Alignment Algorithm*” [16]. This alignment is suboptimal from the perspective of regression, since the response variable is not used in this phase-amplitude separation.

Nonparametric Kernel Approach. As mentioned earlier, one can use the Nadaraya-Watson estimator (of the kind given in Eqn. 4) for predicting y for a new predictor function f . The only quantity left unspecified in that equation is the metric structure

on \mathcal{F} . In the following we choose the distance to be: $d(f, f_i) = \lambda d_a(f, f_i) + (1 - \lambda) d_p(f, f_i)$, where $\lambda \in [0, 1]$ is a proportion parameter. Here d_a denotes the amplitude distance: $d_a(f, f_i) = \operatorname{argmin}_{\gamma \in \Gamma} \|f - (f_i * \hat{\gamma}_i)\|$, where $\hat{\gamma}_i$ is the optimal γ_i obtained by using phase-amplitude separation algorithm [16] and d_p denotes the phase distance: $d_p(f, f_i) = \|\sqrt{\hat{\gamma}} - \sqrt{\hat{\gamma}_i}\|$. The optimal value of the bandwidth \hat{b} can be obtained via cross-validation:

$$\hat{b} = \operatorname{argmin}_{b \in \mathbb{R}_+} \sum_{i=1}^n (y_i - G_{(-i)}(f_i))^2, \quad \text{with} \quad G_{(-i)}(f) = \frac{\sum_{j=1, j \neq i}^n y_j K(d(f_j, f))/b}{\sum_{j=1, j \neq i}^n K(d(f_j, f))/b}$$

For the joint estimation of λ and b , we first compute the optimal bandwidth \hat{b} for each $\lambda \in [0, 1]$. Then, we choose the optimal $\hat{\lambda}$ which gives the lowest cross-validation error.

Next, we present experimental results from these and the proposed methods on a number of data sets.

3.1. Simulation Study

In the studies presented in this section, we perform a five-fold cross-validation and compute the mean and standard deviation of root mean square error (RMSE) for predicting the response variable. We use this RMSE for comparing performances of different regression models.

3.1.1. Simulated Data 1

In the first experiment, we simulate $n = 100$ observations using the model stated in Eqn. 5. For the predictors, we use a Fourier basis and random coefficients to form the functions, $f_i^0(t) = c_{i,1}\sqrt{2}\sin(2\pi t) + c_{i,2}\sqrt{2}\cos(2\pi t)$ where $c_{i,1}, c_{i,2} \sim N(0, 1^2)$. Given these functions, we perturb them using random time warpings $\{\gamma_i\}$ to obtain the predictors $\{f_i = (f_i^0 * \gamma_i)\}$. We also simulate the coefficient function β using the same Fourier basis but with a fixed coefficient vector $c_0 = [5, 5, \dots, 5]$. We plug these quantities in the model, use a quadratic polynomial for h , and add independent observation noise, $\epsilon_i \sim N(0, 0.01^2)$, to obtain the responses $\{y_i\}$.

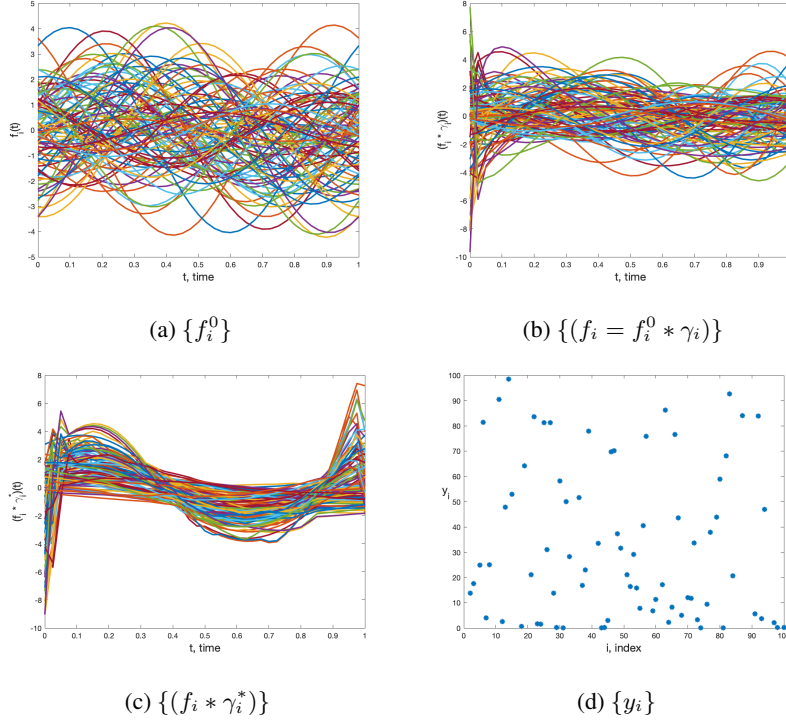


Figure 3: Simulated data 1. (a) shows the original functions, $\{f_i^0\}$, (b) shows them after random warplings, $\{f_i\}$, (c) shows predictors after optimizations over γ_i in the generative model in Eqn. 5, $\{f_i * \gamma_i^*\}$, and (d) displays ordered response variables, $\{y_i\}$, from that model.

Model Estimation. Using the training data, we estimate the model parameters h and β , as described in Algorithm 2. In order to evaluate this algorithm we use three different bases when fitting the model: 1) Fourier basis with only two elements, 2) Fourier basis with four elements, and 3) B-spline basis with four elements. The reason for using different bases for the estimation problem is to study the effects of basis on the model performance. We also try three different polynomials: linear, quadratic, and cubic, for h during estimation.

Fig. 4 shows the evolution of cost function H during optimization in Algorithm 2 for each of index functions: linear, quadratic, and cubic, in Fig. 4a, 4b, and 4c, respectively. These experiments use a Fourier basis with two elements to estimate β . These plots show that the cost function H goes down in all cases and the optimization

algorithm provides at least local solutions reliably. The optimized values are found to be the best for the quadratic and cubic \hat{h} since a quadratic h was used to simulate the data.

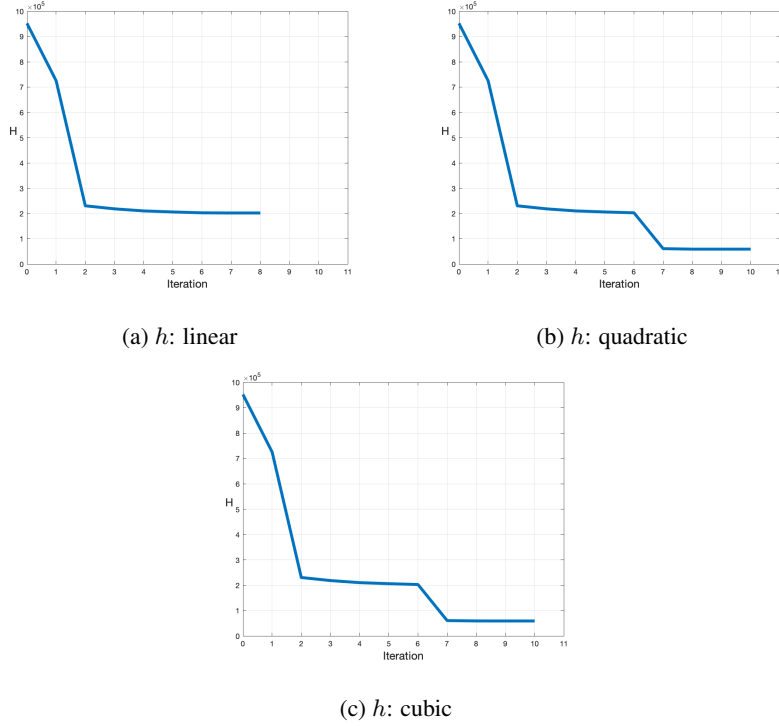


Figure 4: The evolution of cost H for each choice of the index function, h , and using Fourier basis with two elements for β .

It is also important to quantify the estimation errors for model parameters β and h . In order to quantify estimation error, we calculate the Root Squared Error ($\text{RSE}_{\mathbb{L}^2} = \sqrt{\int [\beta(t) - \hat{\beta}(t)]^2 dt}$) for β and Root Mean Squared Error ($\text{RMSE}_{\mathbb{L}^2} = \sqrt{\frac{1}{n} \sum_{i=1}^n \int [\gamma_i(t) - \gamma_i^*(t)]^2 dt}$) for the warping functions, γ_i in \mathbb{L}^2 space. We compute the average of $\text{RSE}_{\mathbb{L}^2}$ and $\text{RMSE}_{\mathbb{L}^2}$ from five different folds in five-fold cross-validation.

The numerical results of estimation error for β and γ are presented in Table 1. We compare EFRM to PAFLM which also pre-aligns the functional predictor to reduce the phase variability without examining the relationship between the predictors and

Basis	Model	RSE$_{\mathbb{L}^2}$ for β	RMSE$_{\mathbb{L}^2}$ for γ
Fourier2	EFRM	68.636	0.017
	PAFLM	93.728	0.025
Fourier4	EFRM	71.567	0.018
	PAFLM	209.831	0.025
Bspline4	EFRM	91.810	0.012
	PAFLM	119.430	0.015

Table 1: The average of RSE $_{\mathbb{L}^2}$ (Root Squared Error) of true and estimated β and the RMSE $_{\mathbb{L}^2}$ of the true and estimated warping functions in \mathbb{L}^2 space.

response variables. As the results show, the proposed EFRM can provide a better estimation performance for both β and γ than PAFLM model.

Prediction Performance. To evaluate prediction performance of a model, we use the model parameters estimated using the training step for predicting the response variable for the test data. This prediction follows the procedure laid out in Eqn. 6. The predicted responses are then compared with the true responses to quantify the prediction error. We perform five-fold cross-validation to evaluate this error more precisely. Then we compute the average and the standard deviation of RMSE ($= \sqrt{\frac{1}{n} \sum_{i=1}^n (y_i - \hat{y}_i)^2}$) from five different folds and use these quantities to compare different models.

The numerical results for the average of the five-fold RMSEs and corresponding standard deviations are shown in Table 2. As these results show, the proposed EFRM is able to provide a better prediction performance than the competing models despite using very simple tools. The predictions from PAFLM are less accurate since this method pre-aligns functional predictors without considering response variables $\{y_i\}$. The nonparametric regression model using the \mathbb{L}^2 norm shows some improvement in prediction, when compared to FLM and PAFLM, since it is not restricted to linear relationships between the response and functional predictors. However, this model also fail to account for the phase variations and the predictions are found to be less accurate than EFRM.

Parametric			
Basis	Fourier2	Fourier4	Bspline4
h : Linear	53.165 (9.026)	52.730 (11.716)	59.078(8.311)
h : Quadratic	32.160 (9.853)	28.236 (11.932)	50.866 (12.042)
h : Cubic	32.523 (9.052)	28.598 (11.298)	48.116 (8.186)
FLM	70.104 (12.622)	68.248 (11.887)	68.109 (10.561)
PAFLM	122.942 (61.945)	148.307 (82.307)	121.895 (66.840)
Nonparametric			
NP- \mathbb{L}^2	52.928 (6.427)		
NP-elastic	59.394 (10.074)		

Table 2: The average and the standard deviation (in parentheses) of the five RMSEs for three model-based methods on simulated test data.

3.1.2. Simulated Data 2

In the second experiment, we again simulate $n = 100$ observations using the model stated in Eqn. 5, but this time we use a B-spline basis with 20 elements and random coefficients to form the predictor functions. As earlier, we simulate the coefficient function β using the same basis and a fixed coefficient vector. Then we plug these quantities in the model, use a quadratic polynomial function h , and add independent observation noise, $\epsilon_i \sim N(0, 0.01^2)$, to obtain the responses $\{y_i\}$. Skipping further details, we focus directly on prediction performance (using the same B-spline basis with 20 elements).

Prediction Performance. The prediction results are shown in Table 3. Despite increased complexity of predictors, resulting from a larger basis set, EFRM still performs well relative to the competing methods.

A part of the success of the proposed model can be attributed to the fact that the data was indeed simulated from that model itself. Therefore, it is natural that this model does better than others. However, these experiments also point to the robustness of the response variable to random phase variability in the functional predictors. Technically,

	Parametric					Nonparametric	
Model	h : linear	h : quadratic	h : cubic	FLM	PAFLM	NP- L^2	NP-elastic
RMSE	2.073 (0.464)	0.798 (0.262)	0.813 (0.257)	2.770 (0.493)	8.591 (4.329)	1.934 (0.574)	2.228 (0.436)

Table 3: The average and the standard deviation (in parentheses) of the five RMSE’s for three model-based methods on simulated test data

the response is invariant to this phase variability. Additionally, the model benefits from optimization over Γ alongside the estimation of β and h . In this way, the model chooses phases in order to maximize prediction performance.

3.2. Application to Real Data

Next, we study the proposed model on three real data examples. There are several important application areas where functional variables form important predictors for response variables of interest. Examples include biosignals, human anatomy, biochemistry, plant biology, and so on. We take three representative examples from biometrics, chemistry and stock market. The goal in each case is to use shapes of certain functional predictors in prediction of corresponding scalar response variables.

Description of the Data.

1. **Gait in Parkinson’s Disease Data:** First, we use Gait data for analysis in Parkinson’s disease data, taken from the well-known *Physionet* [30] database. The database contains of the *Vertical Ground Reaction Force* (VGRF) records of subjects as they walked at their usual, self-selected pace for approximately two minutes on level ground. A total of eight sensors were underneath each foot measuring force (in Newtons) as a function of time. The outputs of each of these 16 sensors (left: 8 and right: 8) have been digitized and recorded at 100 samples per second. From the original data, we extract a very short segment (the first 1 – 100 time points from 12119 time points) for simplicity and efficiency of computation. Based on demographic information, each patient has his/her own *Timed Up And Go* (TUAG) test which is a simple test used to assess a person’s

mobility and requires both static and dynamic balance (second panel). In statistical analysis, we consider VGRF records as the predictor curves and TUAG as scalar responses with each subject forming an independent observation.

There are three different group of patients in Gait in Parkinson’s disease data. We focus on two groups named “*Ga*” and “*Si*” [31–33] in the dataset to ensure the same demographic information among the participants. This results in a total of 61 functions or curves for the analysis.

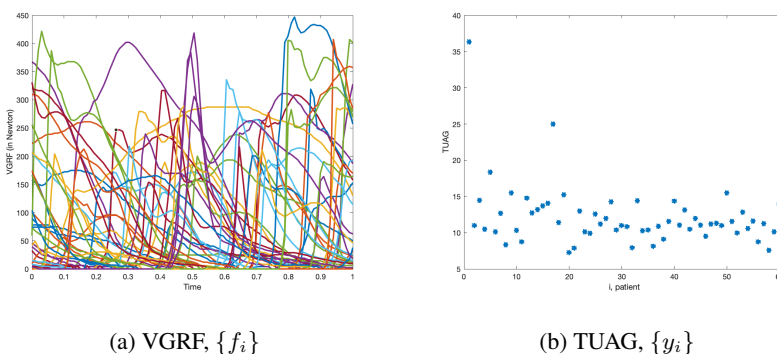


Figure 5: Gait in Parkinson’s Disease Data

Fig. 5 plots the smaller segments of VGRF for each of the 59 patients in the first panel and TUAG values in the second panel. In the experiments presented later, we randomly selected 41 curves as the training set and rest 20 as the test set.

2. **Metabonomic 1H-NMR Data:** Metabonomic 1H-NMR (Nuclear Magnetic Resonance) data [34] originates from 1H NMR analysts of urine from thirty-two rats, fed a diet containing an onion by-product. The aim is to evaluate the *in vivo* metabolome following intake of onion by-products. The data set contains 31 NMR spectra in the region between (0 – 3000) ppm as predictors and some reference chemical values as responses.

Since we have 31 total observations, we randomly select 21 curves as the training set and rest 10 curves as the test set. Similar to the Gait in Parkinson’s disease data, we extracted the first 300 time points from 29001 time points for efficient computation and statistical analysis. Fig. 6 displays the plots of NMR spectra

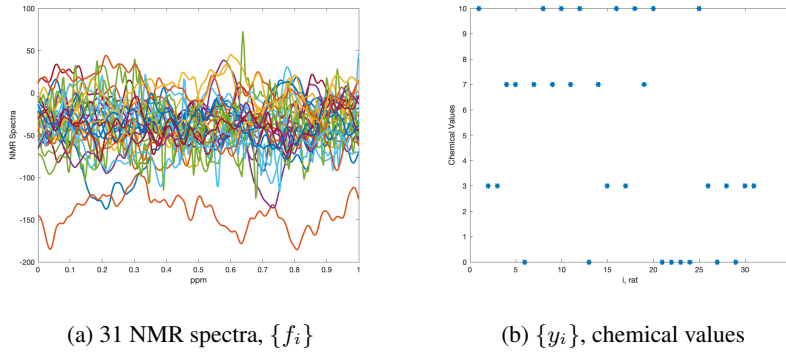


Figure 6: Metabonomic 1H-NMR Data

of 31 rats (first panel) and the chemical values which are considered as response variable (second panel).

3. **Historical Stock Data:** *QuantQuote* has large amount of free historical stock data that is freely available for download from their website. There are total of 200 companies and each company has total 3,926 stock entries during the interval 1/2/1998 to 8/9/2013. For each company, we exported stock prices from 3/20/2012 to 8/9/2012 to form functional predictors. So there are 100 time points over the selected interval for describing the predictor functions. Then, we form the stock prices on 8/9/2013 as the scalar response variable which is exactly one year after the end of interval from predictor (8/9/2012). Hence, our goal is to predict one-year future stock price for each company based on historical stock prices for some interval.

Fig. 7 shows the example of this stock data. The 200 functional predictors are shown in Fig. 7a and scalar response variables are shown in Fig. 7b. We use first 140 curves to fit the model and remaining 60 curves as test.

Analysis of Real Data. For representing the coefficient function β , we used a B-spline basis with 20 elements and estimated parameters using Algorithm 2.

Fig. 8 shows “aligned” functional predictors obtained by warping during the predictor functions at training and testing stages. Each row corresponds to a real data set – gait in Parkinson’s disease (first row), metabonomic 1H-NMR (second row), and

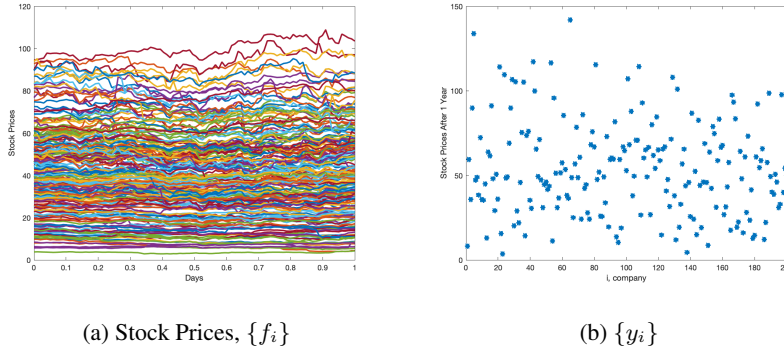


Figure 7: Historical Stock Data

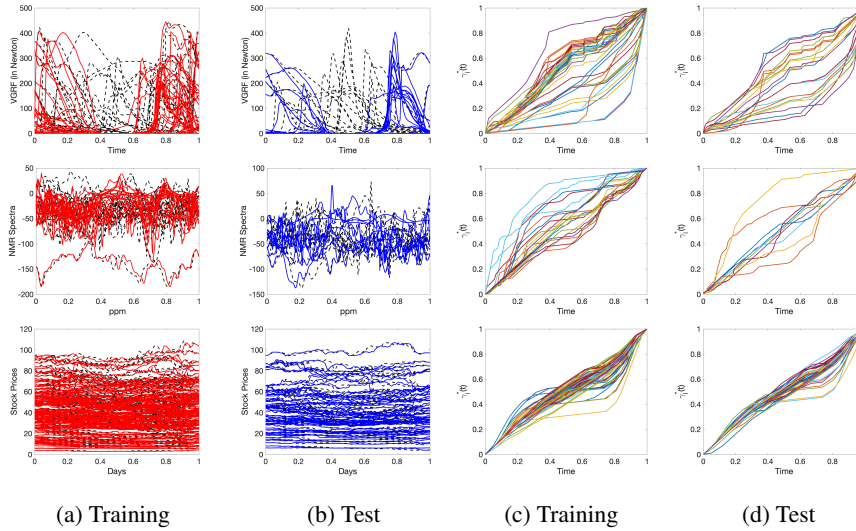


Figure 8: $\{f_i\}$ vs. Warped $\{f_i\}$ and $\{\gamma_i^*\}$

historical stock market (third row). The original functions are drawn in black dashed curves and the warped functions are drawn using the red/blue solid curves. Fig. 8a and 8b show the curves for the training data and the test data, respectively. The corresponding optimal time warping functions, $\{\hat{\gamma}_i\}$ on the training set and the test set are shown in Fig. 8c and 8d, respectively. We remind the readers that the predictors have been warped using the norm-preserving action during the optimization step. They appear more aligned than before but certainly less aligned than those resulting from a pure

alignment algorithm (phase-amplitude separation). We conjecture that this alignment results in an increased ability of the model to predict the response variable. Thus, this warping is more to help regress the responses y_i s to the predictors f_i s, rather than align peaks and valleys in f_i s.

Model	Gait	1H-NMR	Stock
h : Linear	2.707	3.853	8.966
h : Quadratic	2.500	3.825	9.114
h : Cubic	2.617	3.760	9.195
FLM	7.483	226.882	10.405
PAFLM	19.158	43.312	11.086
NP- \mathbb{L}^2	6.559	4.354	9.795
NP-elastic	2.625	4.398	9.540

Table 4: RMSE for predicted response variable under each model.

Prediction Results. Table 4 presents prediction RMSE for each model. It shows that our EFRM model outperforms the other models. Predictions from the kernel regression model are close second to our model, except in the case of stock data. This might be due to the observed functions having all different heights (relatively) and different starting points. Functional predictors in each training data and test data have different shapes (different heights and starting points) so nonparametric method cannot handle this problem. In the case of 1H-NMR data, EFRM using a cubic index function does the best, while in the other cases the lower order polynomials perform slightly better. This could be because the response variable in NMR example is categorical with four values and one needs a cubic polynomial to fit the response levels.

4. Concluding Remarks

The development of a functional regression model that can handle phase variability in functional predictors is a challenging problem in functional data analysis. We have

proposed a new elastic approach uses the shapes of functions, rather than the full functions, as predictors in functional regression model. The notion of shape is based on a norm-preserving warping of the predictors and handles the nuisance phase variability by optimizing the \mathbb{L}^2 inner product over the warping group in the model. We compare the prediction RMSE of the model with several existing methods to demonstrate the effectiveness of this technique using simulated data and real data.

We emphasize that while phase is nuisance in some applications but it is not always the case. One should not expect the *shapes* of predictor functions to be predominant predictors in all situations. Phase components may also carry important information about the responses and one can not always ignore them. However, in some cases, as illustrated through the simulated data and real data examples presented in this paper, shape can be the primary predictor and one wants models that can exploit that knowledge.

As discussed in Section 1.3, there is another model that can potentially eliminate the effects of phase variability in the predictor functional data. This model involves SRVFs $\{q_i\}$ of the predictors and uses the term $\sup_{\gamma_i} \langle (q_i \circ \gamma_i) \sqrt{\gamma_i}, \beta \rangle$ as the argument of the index function h . However, we have pursued is model here because, despite theoretical advantages, the practical performances of this model are sometimes low. As an example, we study the prediction problem using the same stock market data as in item 3 of Section 3.2. The prediction RMSE for this model is listed in Table 5, and is found to be worse than the results shown in Table 4. We conjecture that it is because the noise in predictor data gets enhanced when computing SRVFs (due to the presence of a time derivative in SRVF expression). Thus, we prefer the second option mentioned in Section 1.3 for EFRM.

Model	h : linear	h : quadratic	h : cubic
RMSE	18.032	18.139	18.110

Table 5: RMSEs of using SRVF representation and value-preserving warping.

Acknowledgement

This research was supported in part by the NSF grants NSF-1621787 and NSF-1617397 to AS. This paper describes objective technical results and analysis. Any subjective views or opinions that might be expressed in the paper do not necessarily represent the views of the U.S. Department of Energy or the United States Government. Supported by the Laboratory Directed Research and Development program at Sandia National Laboratories, a multi-mission laboratory managed and operated by National Technology and Engineering Solutions of Sandia, LLC, a wholly owned subsidiary of Honeywell International, Inc., for the U.S. Department of Energy's National Nuclear Security Administration under contract DE-NA0003525.

Availability

MATLAB programs are available upon request.

References

- [1] J. O. Ramsay, B. W. Silverman, [Functional Data Analysis](#), 2nd Edition, Springer, 2005. [doi:10.1007/b98888](#).
- [2] J. S. Morris, [Functional regression](#), *Annual Review of Statistics and Its Application* 2 (2015) 321–359. [doi:10.1146/annurev-statistics-010814-020413](#).
- [3] J. O. Ramsay, C. J. Dalzell, [Some Tools for Functional Data Analysis](#), *Journal of the Royal Statistical Society. Series B (Methodological)* 53 (3) (1991) 539–572. [doi:10.1111/j.2517-6161.1991.tb01844.x](#).
- [4] H. Cardot, F. Ferraty, P. Sarda, [Functional linear model](#), *Statistics & Probability Letters* 45 (1) (1999) 11–22. [doi:10.1016/s0167-7152\(99\)00036-x](#).
- [5] K. Ahn, J. D. Tucker, W. Wu, A. Srivastava, [Elastic Handling of Predictor Phase in Functional Regression Models](#), in: *Proceedings of the IEEE Conference on*

- Computer Vision and Pattern Recognition Workshops, 2018, pp. 324–331. doi: [10.1109/cvprw.2018.00072](https://doi.org/10.1109/cvprw.2018.00072).
- [6] G. M. James, [Generalized Linear Models with Functional Predictors](#), Journal of the Royal Statistical Society. Series B (Statistical Methodology) 64 (3) (2002) 411–432. doi:[10.1111/1467-9868.00342](https://doi.org/10.1111/1467-9868.00342).
- [7] P. T. Reiss, J. Goldsmith, H. L. Shang, R. T. Ogden, [Methods for Scalar-on-Function Regression](#), International Statistical Review 85 (2) (2017) 228–249. doi:[10.1111/insr.12163](https://doi.org/10.1111/insr.12163).
- [8] J. Goldsmith, F. Scheipl, [Estimator selection and combination in scalar-on-function regression](#), Computational Statistics & Data Analysis 70 (2014) 362–372. doi:[10.1016/j.csda.2013.10.009](https://doi.org/10.1016/j.csda.2013.10.009).
- [9] K. Fuchs, F. Scheipl, S. Greven, [Penalized scalar-on-functions regression with interaction term](#), Computational Statistics & Data Analysis 81 (2015) 38–51. doi:[10.1016/j.csda.2014.07.001](https://doi.org/10.1016/j.csda.2014.07.001).
- [10] A. Ciarleglio, R. T. Ogden, [Wavelet-based scalar-on-function finite mixture regression models](#), Computational Statistics & Data Analysis 93 (2016) 86–96. doi:[10.1016/j.csda.2014.11.017](https://doi.org/10.1016/j.csda.2014.11.017).
- [11] J. Gertheiss, J. Goldsmith, C. Crainiceanu, S. Greven, [Longitudinal scalar-on-functions regression with application to tractography data](#), Biostatistics 14 (3) (2013) 447–461. doi:[10.1093/biostatistics/kxs051](https://doi.org/10.1093/biostatistics/kxs051).
- [12] T. T. Cai, P. Hall, [Prediction in functional linear regression](#), The Annals of Statistics 34 (5) (2006) 2159–2179. doi:[10.1214/009053606000000830](https://doi.org/10.1214/009053606000000830).
- [13] H. G. Müller, U. Stadtmüller, [Generalized functional linear models](#), The Annals of Statistics (2005) 774–805doi:[10.1214/009053604000001156](https://doi.org/10.1214/009053604000001156).
- [14] J. S. Marron, J. O. Ramsay, L. M. Sangalli, A. Srivastava, [Functional data analysis of amplitude and phase variation](#), Statistical Science 30 (4) (2015) 468–484. doi:[10.1214/15-sts524](https://doi.org/10.1214/15-sts524).

- [15] J. S. Marron, J. O. Ramsay, L. M. Sangalli, A. Srivastava, [Statistics of time warpings and phase variations](#), *Electronic Journal of Statistics* 8 (2) (2014) 1697–1702. doi:10.1214/14-ejs901.
- [16] A. Srivastava, W. Wu, S. Kurtek, E. Klassen, J. S. Marron, [Registration of Functional Data Using Fisher-Rao Metric](#) arXiv:1103.3817.
- [17] J. D. Tucker, W. Wu, A. Srivastava, [Generative Models for Functional Data Using Phase and Amplitude Separation](#), *Computational Statistics & Data Analysis* 61 (2013) 50–66. doi:10.1016/j.csda.2012.12.001.
- [18] J. O. Ramsay, X. Li, [Curve Registration](#), *Journal of the Royal Statistical Society: Series B (Statistical Methodology)* 60 (1998) 351–363. doi:10.1111/1467-9868.00129.
- [19] X. Liu, H. G. Müller, [Functional convex averaging and synchronization for time-warped random curves](#), *Journal of the American Statistical Association* 99 (2004) 687–699. doi:10.1198/016214504000000999.
- [20] A. Srivastava, E. Klassen, [Functional and shape data analysis](#), Springer, 2016. doi:10.1007/978-1-4939-4020-2.
- [21] F. Ferraty, P. Vieu, [Nonparametric functional data analysis: theory and practice](#), Springer Science & Business Media, 2006. doi:10.1007/0-387-36620-2.
- [22] E. A. Nadaraya, [On estimating regression](#), *Theory of Probability & Its Applications* 9 (1) (1964) 141–142. doi:10.1137/1109020.
- [23] T. M. Stoker, [Consistent estimation of scaled coefficients](#), *Econometrica: Journal of the Econometric Society* (1986) 1461–1481 doi:10.2307/1914309.
- [24] A. Ait-Saïdi, F. Ferraty, R. Kassa, P. Vieu, [Cross-validated estimations in the single-functional index model](#), *Statistics* 42 (6) (2008) 475–494. doi:10.1080/02331880801980377.

- [25] P. H. C. Eilers, B. D. Marx, [Flexible Smoothing with B-Splines and Penalties](#), *Statistical Science* (1996) 89–102 [doi:10.1214/ss/1038425655](#).
- [26] C.-R. Jiang, J.-L. Wang, et al., [Functional single index models for longitudinal data](#), *The Annals of Statistics* 39 (1) (2011) 362–388. [doi:10.1214/10-AOS845](#).
- [27] P. H. C. Eilers, B. Li, B. D. Marx, [Multivariate calibration with single-index signal regression](#), *Chemometrics and Intelligent Laboratory Systems* 96 (2) (2009) 196–202. [doi:10.1016/j.chemolab.2009.02.001](#).
- [28] Y. Li, N. Wang, R. J. Carroll, [Generalized functional linear models with semiparametric single-index interactions](#), *Journal of the American Statistical Association* 105 (490) (2010) 621–633. [doi:10.1198/jasa.2010.tm09313](#).
- [29] J. S. Morris, [Functional regression](#), *Annual Review of Statistics and Its Application* 2 (2015) 321–359. [doi:10.1146/annurev-statistics-010814-020413](#).
- [30] A. L. Goldberger, L. A. N. Amaral, L. Glass, J. M. Hausdorff, P. C. Ivanov, R. G. Mark, J. E. Mietus, G. B. Moody, C. Peng, H. E. Stanley, [PhysioBank, PhysioToolkit, and PhysioNet: Components of a New Research Resource for Complex Physiologic Signals](#), *Circulation* 101 (23) (2000) e215–e220. [doi:10.1161/01.cir.101.23.e215](#).
- [31] S. Frenkel-Toledo, N. Giladi, C. Peretz, T. Herman, L. Gruendlinger, J. M. Hausdorff, [Treadmill walking as an external pacemaker to improve gait rhythm and stability in Parkinson’s disease](#), *Movement Disorders* 20 (9) (2005) 1109–1114. [doi:10.1002/mds.20507](#).
- [32] S. Frenkel-Toledo, N. Giladi, C. Peretz, T. Herman, L. Gruendlinger, J. M. Hausdorff, [Effect of gait speed on gait rhythmicity in Parkinson’s disease: variability of stride time and swing time respond differently](#), *Journal of NeuroEngineering and Rehabilitation* 2 (1) (2005) 23. [doi:10.1186/1743-0003-2-23](#).

- [33] G. Yogev, N. Giladi, C. Peretz, S. I. Springer, E. S. Simon, J. M. Hausdorff, [Dual tasking, gait rhythmicity, and Parkinson's disease: which aspects of gait are attention demanding?](#), *European Journal of Neuroscience* 22 (5) (2005) 1248–1256. doi:10.1111/j.1460-9568.2005.04298.x.
- [34] H. Winning, E. Roldán-Marín, L. O. Dragsted, N. Viereck, M. Poulsen, C. Sánchez-Moreno, M. P. Cano, S. Engelsen, [An exploratory NMR nutri-metabonomic investigation reveals dimethyl sulfone as a dietary biomarker for onion intake](#), *Analyst* 134 (11) (2009) 2344–2351. doi:10.1039/b918259d.